

DSCC2014-6022

**ANALYTIC MODELING AND INTEGRAL CONTROL OF HETEROGENEOUS
THERMOSTATICALLY CONTROLLED LOAD POPULATIONS**

Azad Ghaffari

Department of MAE
UC San Diego
La Jolla, CA 92039-0411
Email: aghaffari@ucsd.edu

Scott Moura

Department of Civil and Environmental Engineering
UC Berkeley
Berkeley, CA 94720
Email: smoura@berkeley.edu

Miroslav Krstić

Department of MAE
UC San Diego
La Jolla, CA 92039-0411
Email: krstic@ucsd.edu

ABSTRACT

Thermostatically controlled loads (TCLs) account for approximately 50% of U.S. electricity consumption. Various techniques have been developed to model TCL populations. A High-fidelity analytical model of heterogeneous TCL populations facilitates the aggregate synthesis of power control in power networks. Such a model assists the utility manager to increase the stability margin of the network. The model, also, assists the customer to schedule his/her tasks in order to reduce his/her energy cost. We present a deterministic hybrid partial differential equation (PDE) model which accounts for heterogeneous populations of TCLs, and facilitates analysis of common scenarios like cold load pick up, cycling, and daily and/or seasonal temperature changes to estimate the aggregate performance of the system. The proposed technique is flexible in terms of parameter selection and ease of changing the set-point temperature and deadband width all over the TCL units. We provide guidelines to maintain the numerical stability of the discretized model during computer simulations. Moreover, the proposed model is a close fit to design output feedback algorithms for power control purposes. Our integral output feedback control, designed using the comparison principle, guarantees fast and efficient power tracking for various real-world scenarios. We present simulation results to verify the effectiveness of the proposed modeling and control technique.

INTRODUCTION

Analytical and numerical models of thermostatically controlled loads (TCLs) including heating, ventilation, and air conditioning (HVAC) systems have been developed to study demand

response in power networks [1–14]. One can refer to [12, 14] among the very first reports that used statistical and stochastic analysis to develop an aggregate model of TCLs. The effect of capital stock, lifestyle, usage response, and price impacts on power curves have been studied in [5, 13]. Mortensen and Haggerty [11] present a brief survey on five different TCL modeling techniques developed up to 1990. More recently TCL modeling has gained extensive attention [1–4, 6–10].

Coupled Fockker-Planck equations (CFPE), derived in [12], present statistical aggregate electrical dynamics for a homogeneous group of devices. A perturbation analysis yields the dynamics for a non homogeneous group. Equations (10)–(18) of [12] include CFPE, 4 algebraic boundary conditions, and 2 ordinary differential equations to guarantee probability conservation. Moreover, the expectation of the operating state of the homogeneous population is given by another ODE defined by Eqn. (43) in [12]. The proposed model does not provide direct access to manipulate the deadband and set-point temperature which makes the controller design process a hard task to achieve. An exact solution to the CFPE which describes the aggregate behavior of TCL populations is presented in [8]. Also, [8] demonstrates the potential to provide ancillary services by remotely manipulating thermostat set-points, particularly to balance fluctuations from intermittent renewable generators.

Another statistical model based on the “state bin transition model” has been developed in [10], a formal abstraction of which is presented in [9] to relax some of the assumptions in [10]. These statistical group of models rely highly on the probability analysis and distribution functions of the TCL population.

A simpler deterministic model with ability to manipulate the set-point temperature using sliding mode control (SMC) has been presented in [1] which overcomes the difficulties attached with statistical modeling and control techniques. The authors propose 2 averaged transport PDEs coupled on the deadband boundaries to model the number of on and off units. Using finite differentiation, the authors present bilinear dynamics for the purpose of power control. The model of [1] does not account for the effect of heterogeneity in TCL populations.

Moura et al. [2] uses diffusion-advection PDEs to simulate the damping effect of heterogeneous populations in the power consumption curve. Also the latter paper presents a distributed identification technique to estimate the parameters of the diffusion-advection PDEs. The diffusion-advection model of [2] is developed based on a phenomenological observation and it requires tuning the diffusion coefficient. On the contrary, our proposed analytical model captures the TCL population power dynamics using the system physical characteristics and it requires no tuning.

We highlight our objectives as follows: i) We develop analytical deterministic PDE dynamics for heterogeneous TCL populations which precisely simulate power changes under temperature fluctuation as happens in the real-world. We parametrize the dynamics of the TCL units such that the units with the same dynamics share 4 transport PDEs coupled through 4 algebraic boundary conditions on 4 different temperature levels. ii) We provide guidelines to guarantee the numerical stability of the discretized dynamics. iii) We design an integral output feedback control such that the system tracks a defined power curve regardless of environmental temperature variation. We actuate the set-point temperature which is a common input for all the TCLs.

Because of its ability to estimate the power consumption dynamics, the proposed model could be augmented to load management programs. Also, one can use the proposed model to study power control via price incentives or to analyze the impact of various demand response policies. Moreover, we show that the linear integral output feedback governs the aggregate power fast enough to an arbitrary level provided that the integrator gain is selected properly. We present different numerical simulations to verify the effectiveness of the proposed modeling and control technique.

The rest of this paper is organized as follows: Section presents the model development. Section describes the output feedback law and provides stability analysis of the power control loop. The simulation results are given in Section . Section concludes the paper.

AGGREGATE PDE-BASED MODEL

The operating state of an individual TCL is controlled by a thermostat whose state depends on temperature. It can be modeled as a hybrid system including one continuous state, temper-

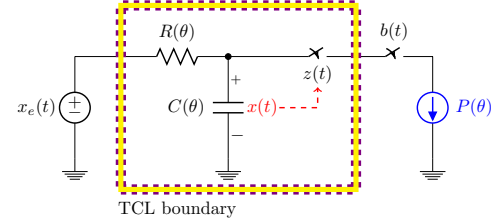


FIGURE 1: EQUIVALENT ELECTRICAL CIRCUIT OF TCL

ature, and a discrete state, operating status e.g. cooling or heating, as introduced in [14]. We consider the heterogeneity effect by parametrizing the physical characteristics of the TCL units, meaning that we have a number of homogeneous TCL groups.

Assume that the temperature of TCL unit j in group i and environmental temperature are x_{ij} and x_e , respectively. As shown in Fig. 1, each TCL unit is modeled as a thermal capacitance, $C_i(\theta_i)$ kWh/°C, in series with a thermal resistance, $R_i(\theta_i)$ °C/kW, all parametrized by θ_i for $i = 1, 2, \dots, m$. The discrete state z_{ij} , modeled by a Schmitt trigger switch shown in Fig. 2, denotes whether the load is on or off. The power injected to each unit in TCL group i is $P_i(\theta_i)$ kW which is also parametrized by θ_i . We assume that m is large enough such that $R(\theta)$, $C(\theta)$, and $P(\theta)$ can be replaced by a continuous approximation, which we assume is also differentiable with respect to θ . To visualize this assumption, we show the sample functions of the system parameters in Fig. 3. We remind the reader that θ is an auxiliary spatial parameter which distinguishes homogeneous populations in our PDE analysis. If the continuity assumption fails, one has to switch to discrete spatial analysis over θ in order to design a control algorithm.

The hybrid dynamics of unit j in TCL group i for a cooling system are defined as follows

$$\frac{dx_{ij}(t)}{dt} = \frac{x_e(t) - x_{ij}(t) - z_{ij}(t)b_i(t)R_i(\theta_i)P_i(\theta_i)}{R_i(\theta_i)C_i(\theta_i)} \quad (1)$$

$$z_{ij}(t) = \begin{cases} 1 & x_{ij}(t - dt) \geq x_H \\ z_{ij}(t - dt) & x_L < x_{ij}(t - dt) < x_H \\ 0 & x_{ij}(t - dt) \leq x_L \end{cases}, \quad (2)$$

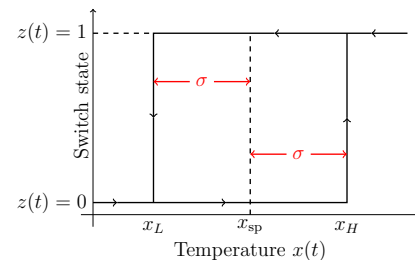


FIGURE 2: SCHMITT TRIGGER SWITCH

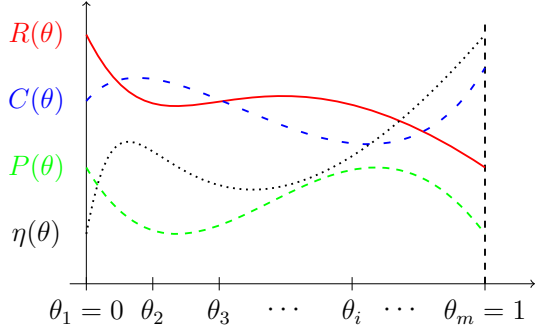


FIGURE 3: SAMPLE FUNCTIONS OF TCL PHYSICAL CHARACTERISTICS VERSUS θ

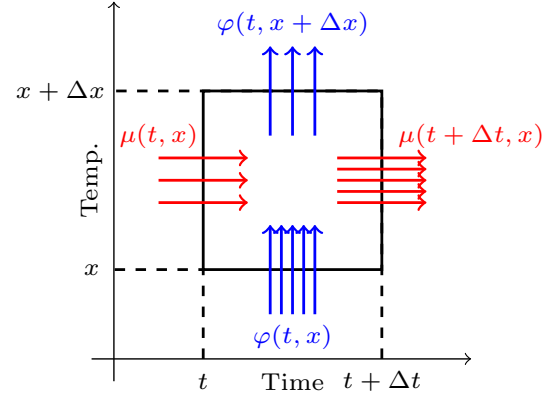


FIGURE 5: VARIATION OF HOMOGENEOUS TCL FLUX OVER INFINITESIMAL TIME-TEMPERATURE WINDOW

for $i = 1, 2, \dots, m$ and $j = 1, 2, \dots, n_i$, where $x_L = x_{sp} - \sigma$ and $x_H = x_{sp} + \sigma$, where x_{sp} is the set-point temperature and 2σ is the deadband width. We assume x_{sp} and σ are the same for the entire TCL population. The utility manager has the ability to override the control system by turning off the main supply switch, $b_i(t) = 0$. We assume that $b_i(t)$ is normally closed, $b_i(t) = 1$. The aggregate power is given by

$$y(t) = \sum_{i=1}^m \left(\frac{P_i(\theta_i)}{\eta_i(\theta_i)} b_i(t) \sum_{j=1}^{n_i} z_{ij}(t) \right), \quad (3)$$

where $\eta_i(\theta_i)$ is the performance coefficient for TCL group i .

We assume that geographical proximity is satisfied which means that the electric loads to be aggregated belong to a geographic area small enough for environmental temperature to be identical. We assume $x \in [x_{min}, x_{max}]$, where the lowest and highest feasible temperature is shown by x_{min} and x_{max} , respectively. As shown in Fig. 4, we select a homogeneous population of TCLs, fixed θ , that have identical hybrid dynamics (1) and (2) and are subject to the same control within a load management program, the same $b_i(t)$ [12]. The density of the TCL units per temperature is a distribution over θ . This distribution is shown by $\mu_{kl}(t, x, \theta)$ to identify on and off TCL units in regions a, b , and c , where $kl = 1a, 1b, 0b, 0c$.

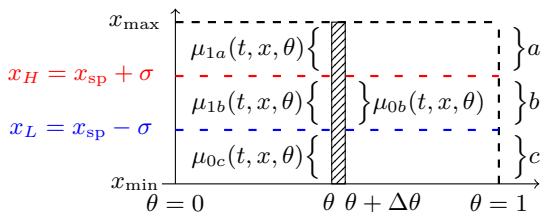


FIGURE 4: DISTRIBUTION FUNCTIONS OF TCLS IN THREE REGIONS

Since θ is fixed, from this point forward we drop θ from the distribution function. The flux of the TCLs which indicates the number of TCLs per second for every $\theta \in [0, 1]$ is obtained as follows

$$\varphi(t, x) = \mu(t, x) \frac{\Delta x}{\Delta t}. \quad (4)$$

Taking the limit of the above equation when $\Delta t \rightarrow 0$ and using (1) gives

$$\varphi(t, x) = \mu(t, x) \frac{x_e(t) - x - zbRP}{RC}. \quad (5)$$

As shown in fig. 5, the total rate of variation of TCLs in a time-temperature window is zero for every $\theta \in [0, 1]$ then

$$\frac{\mu(t + \Delta t, x) - \mu(t, x)}{\Delta t} + \frac{\varphi(t, x + \Delta x) - \varphi(t, x)}{\Delta x} = 0. \quad (6)$$

Taking the limit of the above equation when $\Delta t \rightarrow 0$ and $\Delta x \rightarrow 0$ and using (5) we obtain

$$\frac{\partial \mu(t, x)}{\partial t} = -\frac{\partial}{\partial x} \left(\mu(t, x) \frac{x_e - x - zbRP}{RC} \right) \quad (7)$$

which defines the system dynamics of the TCLs in all regions of Fig. 4

$$\frac{\partial \mu_{kl}(t, x, \theta)}{\partial t} = -\frac{\partial}{\partial x} \left(\mu_{kl}(t, x, \theta) \frac{x_e - x - kbR(\theta)P(\theta)}{R(\theta)C(\theta)} \right), \quad (8)$$

where $kl = 0c, 0b, 1b, 1a$. We need 4 boundary conditions to solve the dynamics equations of (8). The flux is conserved at x_H and x_L

$$\varphi_{0b}(t, x_H, \theta) + \varphi_{1b}(t, x_H, \theta) = \varphi_{1a}(t, x_H, \theta) \quad (9)$$

$$\varphi_{0b}(t, x_L, \theta) + \varphi_{1b}(t, x_L, \theta) = \varphi_{0c}(t, x_L, \theta), \quad (10)$$

then using (5) we obtain

$$\mu_{1b}(x_H) = \mu_{1a}(x_H) + m_{\text{on}}\mu_{0b}(x_H) \quad (11)$$

$$\mu_{0b}(x_L) = \mu_{0c}(x_L) + m_{\text{off}}\mu_{1b}(x_L) \quad (12)$$

for all $t \in [0, \infty)$ and $\theta \in [0, 1]$, where

$$m_{\text{on}} = -\frac{x_e - x_H}{x_e - x_H - RP} > 0 \quad (13)$$

$$m_{\text{off}} = -\frac{x_e - x_L - RP}{x_e - x_L} > 0. \quad (14)$$

Also, at x_{max}^+ and x_{min}^- the following conditions are valid

$$\mu_{1a}(x_{\text{max}}^+) = 0 \quad (15)$$

$$\mu_{0c}(x_{\text{min}}^-) = 0 \quad (16)$$

for all $t \in [0, \infty)$ and $\theta \in [0, 1]$. The system of (8) along with (11), (12), (15), and (16) define the evolution of TCLs over time and temperature for every $\theta \in [0, 1]$. The number of on units per θ equals

$$\rho(t, \theta) = \int_{x_L}^{x_H} \mu_{1b}(t, x, \theta) dx + \int_{x_H}^{x_{\text{max}}} \mu_{1a}(t, x, \theta) dx, \quad (17)$$

and the power consumption for the entire TCL population is calculated as

$$y(t) = \int_0^1 \frac{P(\theta)}{\eta(\theta)} \rho(t, \theta) d\theta. \quad (18)$$

For simulation purposes, we suggest the reader to use the forward and backward finite difference methods for on and off units, respectively. However, care has to be taken that the population of the TCL units remains unchanged during the numerical simulation. Since the units in regions a and c eventually enter the deadband, we need to make sure that the population rollover between on and off units forced by the boundary conditions (11) and (12) introduce a pole at zero to guarantee an unchanged TCL

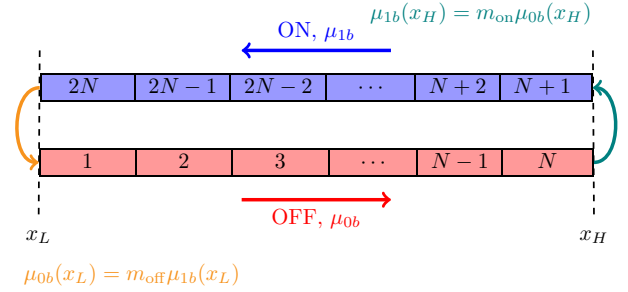


FIGURE 6: METHOD OF FINITE DIFFERENCE

population. As shown in Fig. 6, we divide the deadband region into N equal temperature bin, Δx . By applying the method of finite difference to (8) for on and off units in region b we get

$$\frac{d\mu_2}{dt} = (\alpha - \alpha_2)\mu_2 + \alpha_2\mu_1 \quad (19)$$

$$\frac{d\mu_i}{dt} = (\alpha - \alpha_i)\mu_i + \alpha_i\mu_{i-1} \quad (20)$$

$$\frac{d\mu_{N+2}}{dt} = (\alpha - \alpha_{N+2})\mu_{N+2} + \alpha_{N+2}\mu_{N+1} \quad (21)$$

$$\frac{d\mu_{N+i}}{dt} = (\alpha - \alpha_{N+i})\mu_{N+i} + \alpha_{N+i}\mu_{N+i-1}, \quad (22)$$

where $i = 3, 4, \dots, N$, $\mu_1 = m_{\text{off}}\mu_{2N}$, $\mu_{N+1} = m_{\text{on}}\mu_N$, $\alpha = 1/(RC)$, and

$$\alpha_i = \frac{x_e - x_i}{RC\Delta x} > 0, \quad i = 2, 3, \dots, N \quad (23)$$

$$\alpha_i = \frac{x_i + RP - x_e}{RC\Delta x} > 0, \quad i = N+2, N+3, \dots, 2N. \quad (24)$$

Also, $\alpha_i - \alpha > 0$ for all $i \in \{2, 3, \dots, 2N\} - \{N+1\}$. The characteristic equation of the system dynamics equals

$$\prod_{\substack{i=2 \\ i \neq N+1}}^{2N} (s + \alpha_i - \alpha) - m_{\text{on}}m_{\text{off}} \prod_{\substack{i=2 \\ i \neq N+1}}^{2N} \alpha_i = 0. \quad (25)$$

Occurrence of one eigenvalue at zero is guaranteed if m_{on} and m_{off} are redefined as follows

$$m'_{\text{on}} = \kappa m_{\text{on}} \quad (26)$$

$$m'_{\text{off}} = \kappa m_{\text{off}}, \quad (27)$$

where

$$\kappa = \prod_{\substack{i=2 \\ i \neq N+1}}^{2N} \sqrt{\frac{\alpha_i - \alpha}{\alpha_i m_{\text{on}} m_{\text{off}}}}. \quad (28)$$

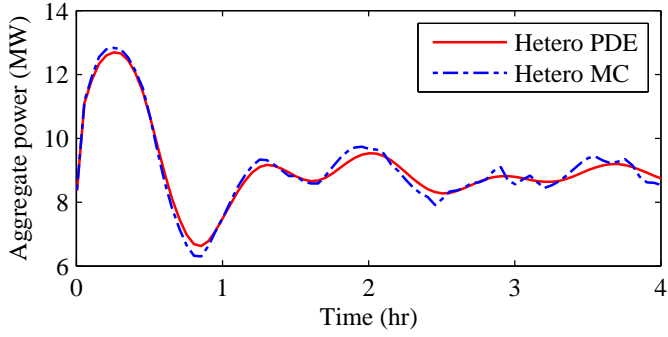


FIGURE 7: STEP RESPONSE FOR (SOLID RED) OUR PROPOSED PDE-BASED AND (DASHED BLUE) MONTE CARLO MODEL

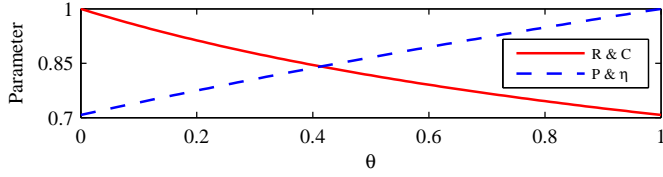


FIGURE 8: NORMALIZED PHYSICAL PARAMETERS

Remark 1. One requires the discretized model to retain a “conservation of matter” property, meaning that the TCLs don’t disappear or appear over time. This mathematically means the discretized equations should have a pole at the origin. Since the TCL population is not changing, when numerical simulations based on the finite difference method are conducted, the boundary conditions of (11) and (12) need to be corrected by replacing (13) and (14) with (26) and (27), respectively. The corrector κ defined by (28) guarantees that a pole happens at zero at each time step and the TCL population remains unchanged during the course of simulation.

Figure 7 shows the system response to a step change in the set-point temperature from 24.5 °C to 24 °C with $\sigma = 1$ °C. The proposed PDE-based model accurately captures the power dynamics of a heterogeneous population of TCL units. We compare our aggregate model (8) against a Monte Carlo model of 40,000 heterogeneous TCLs generated from (1) and (2) distributed evenly between on and off units in the deadband in 10 groups over $0 \leq \theta \leq 1$. The characteristic parameters are defined as $R(\theta) = R_0 f(\theta)$, $C(\theta) = C_0 f(\theta)$, $P(\theta) = P_0 / f(\theta)$, and $\eta(\theta) = \eta_0 / f(\theta)$, where $R_0 = 2$ °C/kW, $C_0 = 1$ kWh/°C, $P_0 = 10$ kW, $\eta_0 = 2.5$, and $f(\theta) = \sqrt{2/(1+\theta)}$ is an arbitrary continuous function with continuous first order derivative for $\theta \in [0, 1]$. The normalized parameters are shown in Fig. 8. Tem-

perature values are given as $x_{sp} = 24$ °C, $\sigma = 1$ °C, $x_e = 35$ °C. Since smaller RC means fast power dissipation, we choose $P(\theta)$ varying in the opposite direction of R and C . Also, for simplicity, we chose the power efficiency to be the same all over the TCL groups and equal $P/\eta = 4$.

In the next section we use the proposed model to design a reference tracking control to achieve power control in heterogeneous TCL populations.

CONTROL DESIGN AND STABILITY ANALYSIS

While the control actuators are distributed across the TCL units, a supervisory system can manipulate the set-point temperature and deadband width of the switches to control the aggregate power consumption. The deadband width changes the power consumption curve to a lower extent. Sudden increases in power demand caused by dramatic fluctuation in environmental temperature or high transient peaks after power outage periods could potentially put the entire system at risk. Hence, the presence of a power control algorithm is necessary.

Various control algorithms for TCLs have been reported in the literature [1, 4, 8, 10]. Bashash and Fathy [1] reported aggregate power control using a sliding mode control algorithm. Their proposed algorithm is based on simplified PDEs with averaged parameters for homogeneous TCL populations. Here, we show that a linear integral output feedback applied to the set-point temperature guarantees fast tracking of reference power provided that the integrator gain is selected properly. Our control is designed based on the coupled transport PDE model of (8), obtained for an arbitrary large number of heterogeneous TCLs, with the boundary conditions of (11), (12), (15), and (16).

Using (17) and denoting the flux equation of (5) on x_H and x_L boundaries, we can calculate the variation of the number of on units versus time as follows

$$\frac{d\rho}{dt} = \varphi_{0b}(x_H) + \varphi_{1b}(x_L) - \mu_{0b}(x_H)\dot{x}_H - \mu_{1b}(x_L)\dot{x}_L. \quad (29)$$

The number of off units turning on equals $\varphi_{0b}(x_H)$ and the number of on units turning off equals $-\varphi_{1b}(x_L)$. The last 2 terms are added to consider the effect of time varying set-point temperature. Assume the switch deadband, σ , is fixed, and the rate of the set-point temperature is controlled by input u

$$\dot{x}_{sp} = u. \quad (30)$$

We use (29) to calculate the time derivative of the consumed power (18)

$$\dot{y} = -c_1(t)u - c_2(t)x_{sp} + c_3(t)\sigma + c_4(t), \quad (31)$$

where

$$c_1(t) = \int_0^1 \frac{P}{\eta} \left(\mu_{1b}(t, x_L, \theta) + \mu_{0b}(t, x_H, \theta) \right) d\theta \quad (32)$$

$$c_2(t) = \int_0^1 \frac{P}{\eta RC} \left(\mu_{1b}(t, x_L, \theta) + \mu_{0b}(t, x_H, \theta) \right) d\theta \quad (33)$$

$$c_3(t) = \int_0^1 \frac{P}{\eta RC} \left(\mu_{1b}(t, x_L, \theta) - \mu_{0b}(t, x_H, \theta) \right) d\theta \leq c_2(t) \quad (34)$$

$$c_4(t) = \int_0^1 \frac{P}{\eta RC} \left((x_e(t) - RP) \mu_{1b}(t, x_L, \theta) + x_e(t) \mu_{0b}(t, x_H, \theta) \right) d\theta \leq x_e(t) c_2(t). \quad (35)$$

Note that $c_1(t)$ indicates the accumulated absolute power variation on the switch boundaries and it is positive and bounded under normal working conditions

$$L_1 \leq c_1(t) \leq U_1, \quad (36)$$

where L_1 and U_1 are positive finite numbers. Given $RC \geq L_\tau > 0$, we can show that $c_2(t)$ is bounded

$$0 < |c_2(t)| \leq \frac{U_1}{L_\tau}. \quad (37)$$

Let y_r and $e = y - y_r$ be the reference power and reference tracking error, respectively. Define the output feedback

$$u(t) = \gamma e(t), \quad (38)$$

where $\gamma > 0$. The error dynamics become

$$\dot{e}(t) = -\gamma c_1(t)e(t) + c_4(t) + \sigma c_3(t) - x_{sp}c_2(t) - \dot{y}_r \quad (39)$$

which gives

$$\begin{aligned} \frac{d}{dt}|e| &= -\gamma c_1|e| + \left(c_4 + \sigma c_3 - x_{sp}c_2 - \dot{y}_r \right) \text{sign}(e) \\ &\leq -\gamma c_1|e| + |c_4 + \sigma c_3 - x_{sp}c_2 - \dot{y}_r| \\ &\leq -\gamma c_1|e| + |c_2||x_e - x_{sp} + \sigma| + |\dot{y}_r|, \end{aligned} \quad (40)$$

where $|e(t)|$ is the absolute value of the error. We assume

$$|x_e - x_{sp} + \sigma| \leq U_x \quad (41)$$

$$|\dot{y}_r| \leq U_y, \quad (42)$$

where U_x , and U_y are finite positive numbers. Using (36), (37), (41), and (42) we rewrite (40) as follows

$$\frac{d}{dt}|e| \leq -\gamma L_1|e| + \frac{U_1 U_x}{L_\tau} + U_y, \quad (43)$$

and by applying the comparison principle [15] we get

$$|e(t)| \leq |e(0)| \exp(-\gamma L_1 t) + \left(\frac{U_1 U_x}{L_1 L_\tau} + \frac{U_y}{L_1} \right) \frac{1}{\gamma}. \quad (44)$$

Note that $U_1 U_x / (L_1 L_\tau) + U_y / L_1$ is of the order of $O(1)$ and (44) is simplified as

$$|e(t)| \leq |e(0)| \exp(-\gamma L_1 t) + O\left(\frac{1}{\gamma}\right). \quad (45)$$

If the feedback gain, $\gamma > 0$, is large enough, then the error settles down to a small neighborhood around zero and reference tracking is achieved. The inverse of γ defines the neighborhood width. Higher feedback gains reduce the steady state error. However, a large feedback gain may drive the set-point temperature outside the working region of $[x_{\min}, x_{\max}]$, particularly in response to large step changes in the reference power. Also, large feedback gains create chattering around the reference power during steady state. Hence, we suggest the reader to select the feedback gain moderately with respect to the reference power and environmental temperature variation.

The proposed control of (38) sacrifices the tracking precision in favor of the simplicity of control design and implementation. One may use a complex state feedback control to achieve perfect reference tracking. However, closed-loop performance improvement and difficulties attached with implementing a state feedback control, which requires a considerable amount of temperature measurement, do not justify the idea of a state feedback control.

The stability proof of the system dynamics is out of the focus of this work and will not be considered here. Nevertheless, intuitively, we know the system dynamics (8) in combination with (11), (12), (15), and (16) are stable for every $x_{sp} \in [x_{\min}, x_{\max}]$.

We summarize the results of power control design in the following theorem.

Theorem 1. Consider a heterogenous TCL population modeled by transport PDEs of (8) coupled through the boundary conditions (11), (12), (15), and (16) with power consumption defined as (18). Assume the accumulated absolute power variation at x_L and x_H is bounded by (36) and the reference power, y_r , and environmental temperature, x_e , satisfy (42) and (41), respectively. Also, the time constant of TCLs satisfies $RC \geq L_\tau > 0$. Then, the output feedback control of (38) with $\gamma > 0$ governs the power consumption to an $O(1/\gamma)$ -neighborhood of y_r .

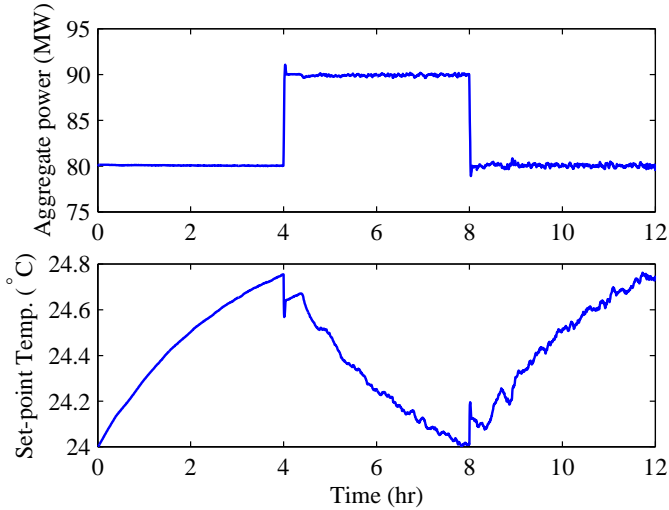


FIGURE 9: REFERENCE TRACKING FOR STEP CHANGES IN POWER LEVEL. (ABOVE) POWER AND (BELOW) SET-POINT TEMPERATURE VARIATION VERSUS TIME

SIMULATION RESULTS

We present simulation results to show the effectiveness of our proposed modeling and control algorithm using the model and parameters presented in Section with $\gamma=0.01$. We assume, at the initial point, all units are located inside the deadband and evenly distributed between on and off states. We use the Monte Carlo model to certify the credibility of the proposed control algorithm.

We present 3 different scenarios in this section: i) Output tracking for step changes in the reference power, ii) Power shaping under daily temperature variation, and iii) Power outage and transient analysis.

Reference tracking performance is shown in Fig. 9 for step changes in power at time $t = 4$ hr from 80 MW to 90 MW and then back to 80 MW at $t = 8$ hr. Due to the slow response time of the system and initial distribution of the on units, set-point temperature varies very slow. The proposed control algorithm updates the set-point temperature slightly at each time step to maintain the power at a fixed level.

Applying a daily environmental temperature curve, as shown in the top part of Fig. 10 for Phoenix, Arizona, from July 13th 6:00 AM until July 14th 6:00 AM, 2013 [16], is a realistic measure to evaluate the performance of our power control technique. We present the response of our proposed control compared to the open-loop scenario in the bottom part of Fig. 10. The controller successively maintains the system at the user defined power shape. Adaptation process of the set-point temperature is shown in Fig. 11. The user can design more sophisticated reference power maps using predictive control algorithms to mitigate both peak power and rate payer discomfort.

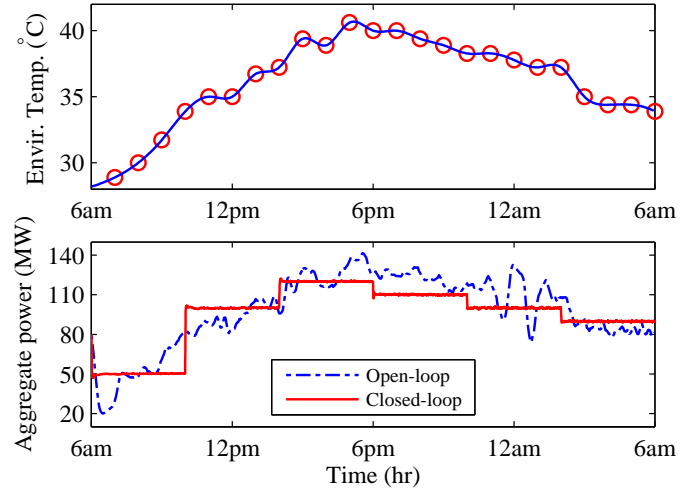


FIGURE 10: (ABOVE) HOURLY VARIATION OF ENVIRONMENTAL TEMPERATURE, (BELOW) VARIATION OF POWER VERSUS TIME FOR (DASHED BLUE) OPEN-LOOP AND (SOLID RED) CLOSED-LOOP SYSTEM

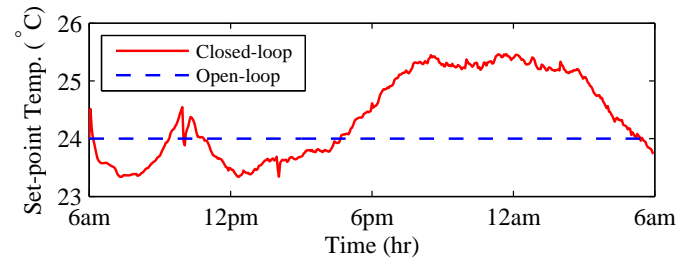


FIGURE 11: SET-POINT EVOLUTION VERSUS TIME

Load management programs could halt the HVACs to alter power flow. The peak power after power restoration could potentially put the system at risk. As shown in the top part of Fig. 12, a half an hour power outage, from $t = 1$ hr to $t = 1.5$ hr, causes all the TCL units to turn on with a slight delay which forces high power demand on the power network. Moreover, the delay location, if matched with the peak demand, creates even more challenges with issues regarding the stability of the power network. Our proposed control dramatically reduces the peak power and governs the system to the reference power by slightly changing the set-point temperature as shown in Fig. 12.

CONCLUSIONS

We modeled heterogeneous populations of thermostatically controlled loads (TCLs) using parametrized transport partial differential equations (PDEs) coupled on the switch deadband

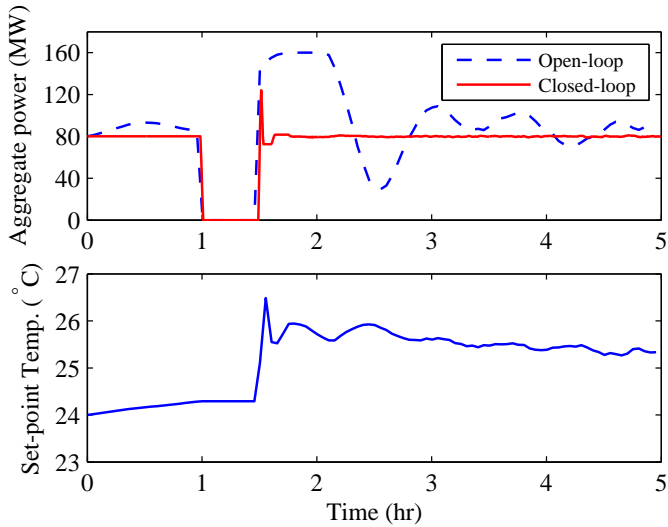


FIGURE 12: (ABOVE) POWER CONSUMPTION FOR (DASHED BLUE) OPEN-LOOP AND (SOLID RED) CLOSED-LOOP SYSTEM, (BELOW) SET-POINT EVOLUTION DURING POWER CONTROL

boundaries. This is the first analytically derived state-space model of heterogeneous TCL populations. The proposed model facilitates the precise simulation of various real life scenarios in heating, cooling, and air conditioning systems. The model uses parametrization to consider the effect of heterogeneity in the physical characteristics of the TCL system. We also investigated the numerical stability of the discretized dynamics. As shown in the reported simulations, the model effectively predicts system performance under daily variation of environmental temperature and power outage enforced by load management programs. Moreover, we showed that the reference power tracking problem for the heterogeneous TCL system can be solved using a linear integrator with a proper gain. The closed-loop stability was investigated using the comparison principle. The simulations were conducted in order to certify the credibility of our proposed modeling and control algorithm in real life scenarios.

REFERENCES

- [1] Bashash, S., and Fathy, H. K., 2013. “Modeling and control of aggregate air conditioning loads for robust renewable power management”. *IEEE Transactions on Control Systems Technology*, **21**, pp. 1318 – 1327.
- [2] Moura, S., Ruiz, V., and Bendtsen, J., 2013. “Modeling heterogeneous populations of thermostatically controlled loads using diffusion-advection PDEs”. In Proc. of ASME Dynamic Systems and Control Conference.
- [3] Moura, S., Bendtsen, J., and Ruiz, V., 2013. “Observer design for boundary coupled PDEs: application to thermostatically controlled loads in smart grids”. In Proc. of IEEE Conference on Decision and Control.
- [4] Zhang, W., J. Lian, C.-Y. C., and Kalsi, K., 2013. “Aggregated modeling and control of air conditioning loads for demand response”. *IEEE Transactions on Power Systems*, **28**, pp. 4655 – 4664.
- [5] Lu, N., and Chassin, D. P., 2004. “A state-queueing model of thermostatically controlled appliances”. *IEEE Transactions on Power Systems*, **19**, pp. 1666–1673.
- [6] Chassin, D. P., and Fuller, J. C., 2011. “On the equilibrium dynamics of demand response in thermostatic loads”. In Proc. of 44th Hawaiian International Conference on System Sciences.
- [7] Kalsi, K., Chassin, F., and Chassin, D., 2011. “Aggregate modeling of thermostatic loads in demand response: a systems and control perspective”. In Proc. of IEEE Conference on Decision and Control and European Control Conference.
- [8] Callaway, D. S., 2009. “Tapping the energy storage potential in electric loads to deliver load following and regulation, with application to wind energy”. *Energy Conversion and Management*, **50**, pp. 1389–1400.
- [9] Soudjani, S. E. Z., and Abate, A., 2013. “Aggregation of thermostatically controlled loads by formal abstractions”. In Proc. of European Control Conference.
- [10] Koch, S., Mathieu, J. L., and Callaway, D. S., 2011. “Modeling and control of aggregated heterogeneous thermostatically controlled loads for ancillary services”. In Proc. of 17th Power Systems Computation Conference.
- [11] Mortensen, R. E., and Haggerty, K. P., 1990. “Dynamics of heating and cooling loads: models, simulation, and actual utility data”. *IEEE Transactions on Power Systems*, **5**, pp. 243–249.
- [12] Malhame, R., and Chong, C.-Y., 1985. “Electrical load model synthesis by diffusion approximation of a high-order hybrid-state stochastic system”. *IEEE Transactions on Automatic Control*, **AC-30**, pp. 854–860.
- [13] Ihara, S., and Schweppe, F. C., 1981. “Physically based modeling of cold load pickup”. *IEEE Transactions on Power Apparatus and Systems*, **PAS-100**, pp. 4142–4150.
- [14] Chong, C. Y., and Debs, A. S., 1979. “Statistical synthesis of power system functional load models”. In Proc. of IEEE Conference on Decision and Control.
- [15] Khalil, H. K., 1996. *Nonlinear Systems*, second ed. Prentice Hall, NJ: Englewood Cliffs.
- [16] wunderground, 2013. “Weather history for Phoenix, AZ”. In <http://www.wunderground.com/history/airport/KPHX/2013/7/13/DailyHistory>.